ACADEMIA ROMÂNĂ
Revue Roumaine de Chimie
https://www.icf.ro/rrch/

Rev. Roum. Chim.,
2024, *69*(3–4), 191–199
DOI: 10.33224/rrch.2024.69.3-4.09

EVALUATING THE CORROSION INHIBITION POTENTIAL OF TWO INNOVATIVE N-BENZYL-5-BROMO ISATIN DERIVATIVES FOR CARBON STEEL IN ALKALINE ENVIRONMENTS: INSIGHTS FROM DFT, SAR AND TOXICOLOGY

Adel KHIOUANI[a*] and Salah Eddine HACHANI[b]

[a]Laboratory of Chemistry of Materials and Living Organisms Activity and Reactivity (LCMVAR), Faculty of Material Sciences, Department of Chemistry, University of Batna 1, Algeria
[b]Department of Process Engineering & Petrochemistry, Faculty of Technology, University of El Oued, El Oued, 39000, Algeria

Received November 9, 2023

DFT-derived global reactivity indices, structure-activity relationships (SAR), and toxicity parameters have been used to correlate between the corrosion inhibition role of two N-benzyl-5-bromo isatin derivatives namely N-benzyl-5-bromo-3-[(imine aceto) urea]-2-oxo indole (ISAO) and N-benzyl-5-bromo-3-[(imine aceto) thiourea]-2-oxo indole (ISAS) against carbon steel corrosion in an alkaline environment and their electronic properties at molecular scale as well as understanding their impacts on human health. The computed global reactivity indices and SAR parameters establish a direct correlation with previously reported experimental data. Mulliken charge analysis provides helpful insights into the atoms responsible for electronic transfer. The predicted toxicological parameters suggest that the tested corrosion inhibitors pose no significant risk to human health.

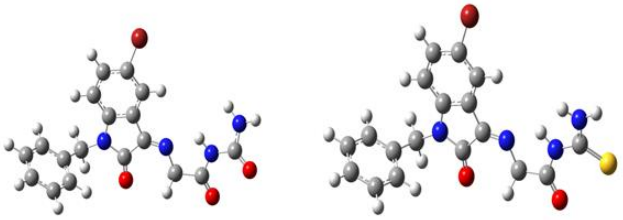

INTRODUCTION

Carbon steel, an iron-based alloy primarily composed of carbon in proportions ranging from 0.12% to 2%, is a widely employed material in the construction of piping and valves within the realms of refineries and petrochemical plants. Its extensive application stems from its economic efficiency.[1] Nonetheless, in offshore settings, carbon steel is susceptible to corrosion from aggressive elements present in oil and gas, notably carbon dioxide (CO_2) and hydrogen sulfide (H_2S), leading to potential economic ramifications.[2]

Organic compounds featuring heteroatoms, conjugated bonds, and planar cycles in their molecular structures have gained significant prominence as highly recommended corrosion inhibitors. Their effectiveness is attributed to their facile adhesion onto metallic substrates through reactions with the corroded metal surface, ultimately forming a protective, ultra-thin layer.[3] This adherence can be accomplished through either chemisorption or physisorption phenomena.[4]

Various techniques such as polarization, electrochemical impedance spectroscopy, and weight loss measurements have been employed to

* Corresponding author: adel.khiouani@univ-batna.dz

assess the corrosion inhibition capabilities of tested chemical compounds for the prevention of carbon steel corrosion. However, these analytical methods are characterized by their substantial cost and time-intensive nature.[5]

In recent years, with significant advancements in computational chemistry and computer technology, this field has emerged as a powerful tool for investigating and comprehensively understanding the corrosion process as an alteration phenomenon, offering insights into effective strategies to safeguard metal surfaces from deterioration.[6]

Density Functional Theory (DFT) has emerged as a highly effective theoretical framework, widely esteemed for its ability to elucidate and provide insights into various experimental findings within the realm of corrosion. Within this context, global reactivity descriptors play a pivotal role by facilitating the establishment of connections between the overall inhibition efficacy of a studied molecule and its electronic attributes. These essential quantum indices encompass a range of parameters, including the energy of the highest occupied molecular orbital, the energy of the lowest unoccupied molecular orbital, electrophilicity, nucleophilicity, dipole moment, hardness, softness, electronegativity, and the fraction of electrons transferred from the inhibitor to the metal.[7]

Structure-Activity Relationship (SAR) analysis stands as a pivotal instrument in the realm of corrosion inhibitors, with the overarching objective of formulating a quantitative connection between the molecular architecture of inhibitor compounds and their manifested inhibitory efficacy against metal corrosion. The insightful SAR analysis contributes significantly by enabling the anticipation of the inhibition efficiency of novel compounds through an evaluation of their structural attributes. Consequently, it serves as an indispensable aid in the judicious and methodical design, as well as the optimization, of corrosion inhibitors.[8]

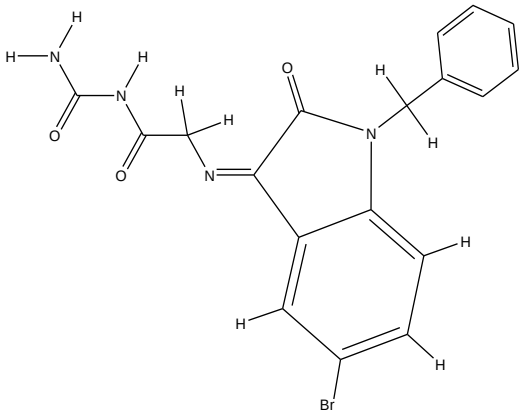

ISAO

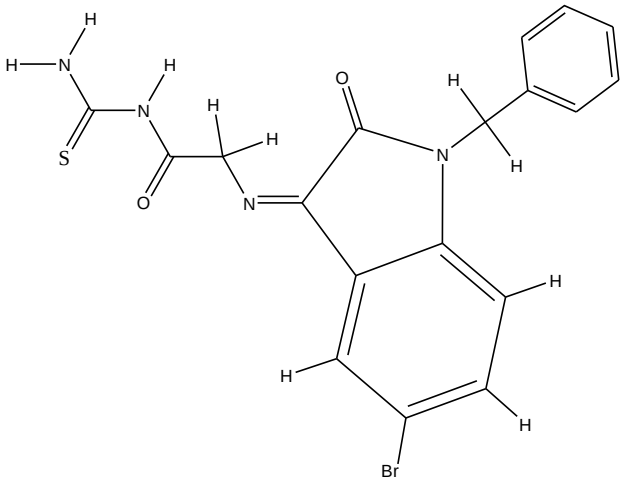

ISAS

Fig. 1 – Molecular structures of the studied isatin derivatives corrosion inhibitors.

The anticipation of corrosion inhibitor toxicity assumes a position of paramount significance, driven by a multitude of compelling motives. Foremost, it plays an indispensable role as a pivotal instrument for upholding environmental integrity and the preservation of human well-being and safety. Beyond its fundamental role, it piques the unwavering enthusiasm of corrosion inhibitor manufacturers who aspire to forge products that transcend mere corrosion control, showcasing a resolute dedication to environmental stewardship and the safeguarding of human health. The prescient insight into toxicity assumes a pivotal role, guiding the meticulous refinement of corrosion inhibitor formulations that steadfastly prioritize safety and sustainability in their composition.[9]

In a comprehensive research study, Rehab M. Kubba and colleagues have successfully synthesized two innovative N-benzyl-5-bromo isatin derivatives, namely N-benzyl-5-bromo-3-[(imine aceto) urea]-2-oxo indole (ISAO) and N-benzyl-5-bromo-3-[(imine aceto) thiourea]-2-oxo indole (ISAS). These novel compounds were meticulously evaluated for their efficacy in protecting carbon steel against corrosion in a 3.5% NaCl solution.[10]

This paper endeavors to make a novel theoretical contribution by harnessing Density Functional Theory (DFT) and Structure-Activity Relationship (SAR) methodologies, aiming to provide a deeper understanding of the intricate interplay between the chemical reactivity of the aforementioned inhibitors and their pivotal roles in corrosion inhibition.

COMPUTATIONAL PART

Geometry optimization

In this investigation, DFT calculations have been meticulously conducted in both the gaseous and aqueous phases, employing the renowned Becke, 3-parameter, Lee-Yang-Par (B3LYP) exchange-correlation density functional,[11] complemented by the highly efficient 6-31G basis set. This rigorous approach was undertaken to establish meaningful correlations between the electronic characteristics of the ISAO and ISAS molecules and their corrosion inhibition properties, with the ultimate goal of unraveling the inhibition mechanism.

The molecular structures of the inhibitors were initially generated in their neutral forms using GaussView 6.0. Subsequently, these structures underwent optimization through the utilization of the Gaussian software package version 3.

Global reactivity descriptors calculation

The resultant theoretical data was harnessed to compute crucial global reactivity descriptors. According to Koopmans' theory, the ionization potential (I) and the electronic affinity (A) were directly derived from the energy values of the Highest Occupied Molecular Orbital (HOMO) and the Lowest Unoccupied Molecular Orbital (LUMO), as elucidated by the following mathematical relationships:[12]

$$I = -E_{HOMO} \quad (1)$$

$$A = -E_{LUMO} \quad (2)$$

Pearson's equations permitting to quantify quantum parameters including electronegativity (χ), the chemical hardness (η) and its inverse; the softness (σ) are given as:[13]

$$\chi = \frac{I + A}{2} \quad (3)$$

$$\eta = \frac{I - A}{2} \quad (4)$$

$$\sigma = \frac{1}{\eta} \quad (5)$$

The fraction of electrons transferred (N) from the inhibitor to mild steel was calculated using Pearson's formula drafted with global hardness and the electronegativity equalization principle:[13]

$$\Delta N = \frac{\chi_{Fe} - \chi_{in}}{2(\eta_{Fe} + \eta_{in})} \quad (6)$$

In the above formula (6), χ_{Fe} and χ_{in} are dedicated both electronegativity of bulk iron and the inhibitor, respectively. η_{Fe} and η_{in} represent the absolute hardness of bulk iron and the inhibitor candidate, respectively, where χ_{Fe} = 7 eV and η_{Fe} = 0 eV.[14]

SAR calculations

In our pursuit of understanding molecular interactions, we conducted a comprehensive analysis of Structure-Activity Relationship (SAR) indices. These indices encompass crucial parameters such as polarizability, surface area, molecular volume, and the partition coefficient Log P. To derive these valuable insights, we

employed the powerful computational tools provided by HyperChem 8.0 software.

Toxicity prediction

To assess the potential effects of the tested corrosion inhibitor compounds on human health, various toxicological parameters such as carcinogenicity, skin sensitization, and AMES toxicity were rigorously computed and predicted using ProTox-II virtual toxicity Lab.

RESULTS AND DISCUSSION

Global reactivity results

The inhibitory performance of two N-benzyl-5-bromo isatin derivatives namely N-benzyl-5-bromo-3-[(imine aceto) urea]-2-oxo indole (ISAO) and N-benzyl-5-bromo-3-[(imine aceto) thiourea]-2-oxo indole (ISAS) against carbon steel corrosion in an alkaline environment was rigorously assessed by several laboratory techniques. The findings of this investigation underscore the remarkable efficacy of these inhibitors in safeguarding carbon steel from the pernicious effects of corrosion. Notably, the experimental inhibition efficiency is observed to follow the order: ISAS > ISAO.[10]

This study endeavors to elucidate the intricate relationship between the experimental inhibitory roles of the scrutinized molecules and their intrinsic properties at the molecular level. In this pursuit, we present comprehensive insights derived from the analysis of global reactivity indices for these compounds, which were meticulously calculated using DFT/B3LYP/6-31G level and then listed in Table 1.

Table 1

Global reactivity descriptors of the studied corrosion inhibitors, calculated at DFT/B3LYP/6-31G theoretical level

Quantum parameter	ISAO	ISAS
μ	10.8750	12.2446
E_{HOMO}	–6.5147	–5.2760
E_{LUMO}	–3.0531	–3.1552
ΔE	3.4616	2.1208
I	6.5147	5.2760
A	3.0531	3.1552
η	1.7308	1.0604
σ	0.5778	0.9430
χ	4.7839	4.2156
ΔN	1.9178	1.4763

Furthermore, we offer a visual representation of the fully optimized molecular structures and the electron distribution within the Highest Occupied Molecular Orbital (HOMO) and Lowest Unoccupied Molecular Orbital (LUMO) frontier orbitals, all elegantly depicted in Fig. 3.

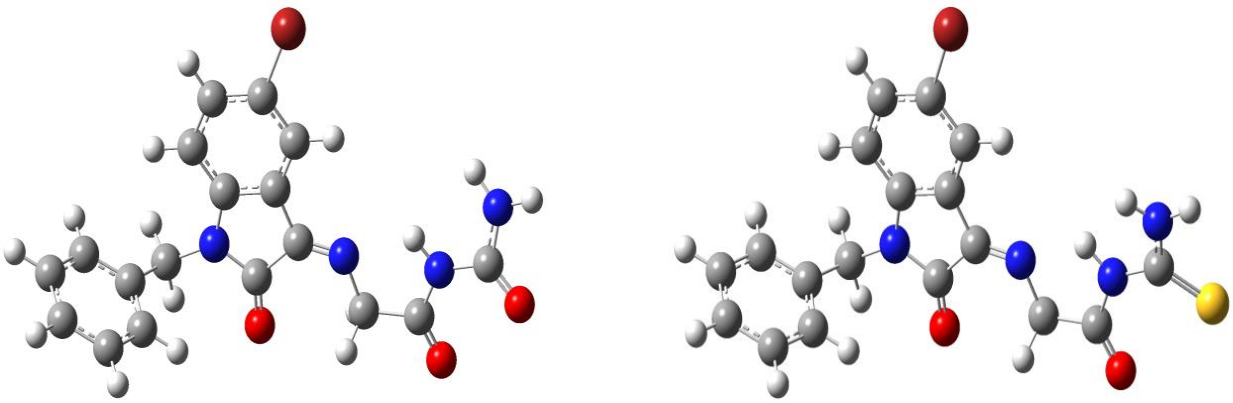

Fig. 2 – Optimized molecular structures of the studied isatin derivatives corrosion inhibitors, calculated at DFT/B3LYP/6-31G theoretical level.

In accordance with the pioneering Frontier Molecular Orbital (FMO) concept introduced by Fukui Kenichi, the process of electron transfer hinges on the dynamic interplay between the highest occupied molecular orbital (HOMO) and the lowest unoccupied molecular orbital (LUMO) of the reacting species.[15] The electron-donating potential of an inhibitor molecule escalates concomitantly with an elevation in its HOMO energy (E_{HOMO}). Consequently, a proclivity towards enhanced inhibition efficacy is anticipated, and as substantiated by the data in Table1, the inhibitor ISAS boasts a higher HOMO energy when compared to ISAO, harmoniously aligning with previous experimental findings.

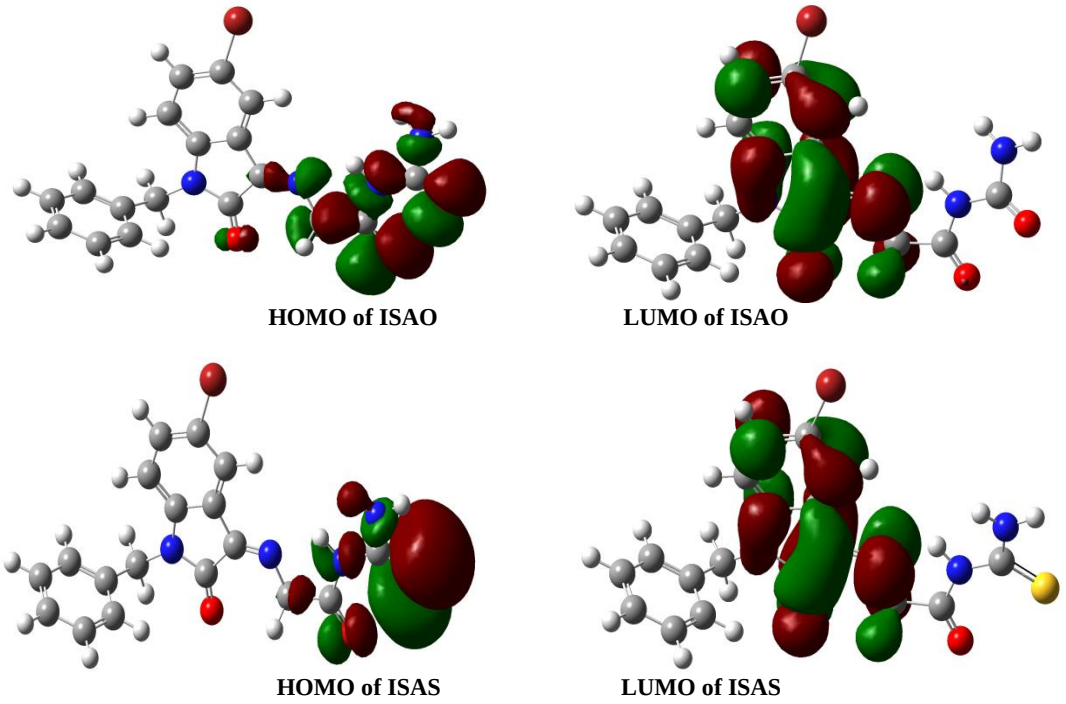

Fig. 3 – HOMO and LUMO electronic localization in the studied isatin derivatives corrosion inhibitors, calculated at DFT/B3LYP/6-31G theoretical level.

Moreover, the assessment of chemical reactivity involves the consideration of a pivotal quantum descriptor known as the energy gap (ΔE), denoting the discrepancy between HOMO and LUMO energy levels.[16] A narrower energy gap is indicative of heightened reactivity and, by extension, superior protection of the metal surface in comparison to other inhibitor compounds. Our theoretical outcomes, as presented in Table 1, clearly demonstrate that the ΔE values for the studied inhibitors adhere to the sequence ISAS > ISAO, in consonance with the experimental observations.

Furthermore, chemical hardness (η) and its reciprocal counterpart, chemical softness (σ), serve as indispensable reactivity indicators. Hardness gauges a molecule's resistance to electron cloud deformation or polarization during a chemical reaction.[17] Molecules characterized by lower chemical hardness values exhibit a robust aptitude for shielding the metal, signifying heightened inhibition efficiency. The results of Table 1 underscores that the chemical hardness for the examined benzoic acid derivatives follows the trend: ISAO > ISAS, while the softness follows the inverse order: ISAS > ISAO. These outcomes consistently mirror the experimental hierarchy of inhibition efficiency.

Electronegativity (χ) emerges as a pivotal quantum index delineating an atom's propensity within a molecule to attract shared electron pairs towards itself.[18] Lower electronegativity is a hallmark of exceptional corrosion inhibitors. As displayed in Table 1, ISAS exhibits a lower electronegativity than ISAO, underscoring the inference that ISAS possesses superior potential to safeguard carbon steel against corrosion, a premise firmly corroborated by experimental observations.

The transfer of electrons, symbolized by ΔN, delineates the number of electrons dispatched from the inhibitor candidate to the carbon steel surface, an indispensable quantum parameter, and integral component of Pearson's equation.[19]A positive ΔN, below the threshold of 3.6, is indicative of the inhibitor's propensity to furnish electrons to the deficient metal surface, thus ensuring maximal protection against corrosion. ΔN data elucidates that the inhibitors under scrutiny function as electron donors to ameliorate the inadequacies of the metal surface, with electron donation increasing in the sequence: ISAS < ISAO, which does not correlate with experimental results.

Lastly, the dipole moment (μ) serves as a harbinger of the polarity inherent to chemical entities. A non-zero dipole moment signifies a molecule's polarity.[19] Moreover, the dipole moment (μ) functions as a valuable reactivity parameter, with higher values indicative of an inhibitor's enhanced affinity to adhere to the metal

surface forming a protective barrier against various corrosive agents. The data in Table 1 unequivocally portrays the rise in dipole moment (μ) values as ISAO < ISAS, mirroring the consistency of these results with experimental observations.

Mulliken charge analysis

Mulliken charge analysis is a quantitative method employed for the distribution of electrons within a molecule. It is based on electronic functions and offers insights into the localization of electrons in a molecule. The Mulliken charge refers to the partial charges assigned to individual atoms within a molecule.[20]

This analysis pertains to the interactions between nuclei and electrophiles, encompassing chemical reactions, particularly in the realm of organic chemistry. Nucleophiles are specific chemical entities that exhibit an affinity for electron-rich sites and can form attachments with them. Nucleophiles typically bear a surplus of negative electrical charges, contrasting with electron-rich atoms like halogens. Electrophiles, on the other hand, feature atoms with partial positive charges or polar bonds.[20]

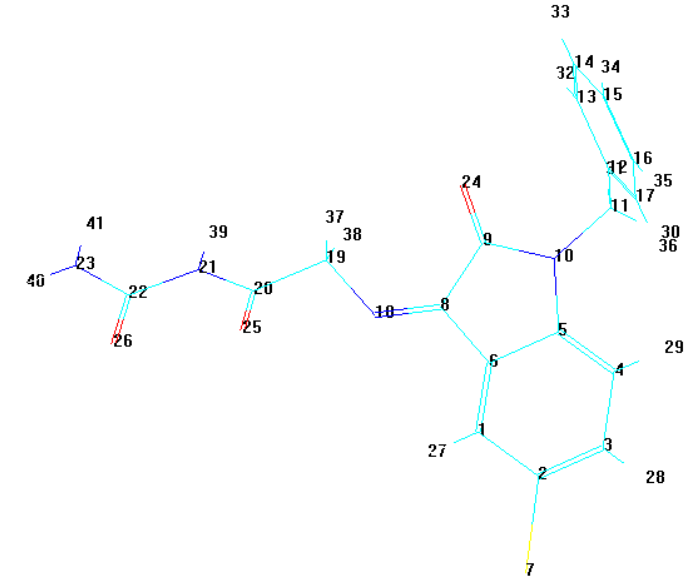

ISAO

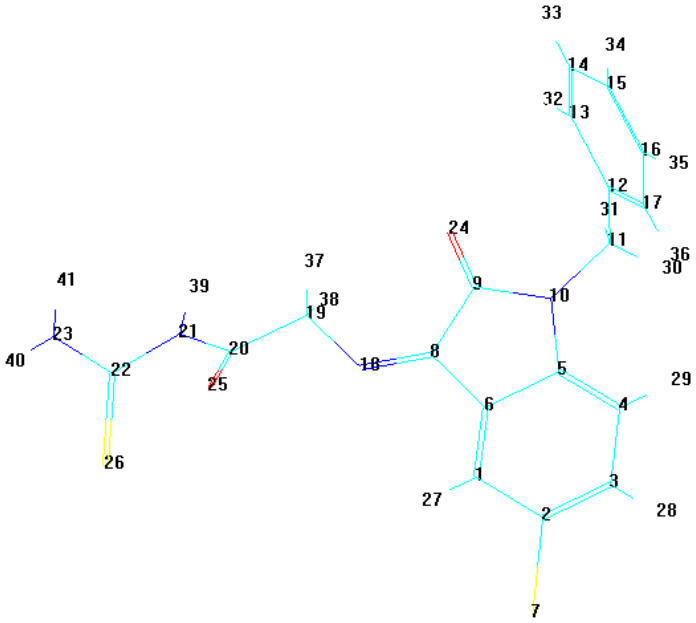

ISAS

Fig. 4 – The atomic numbering of the examined corrosion inhibitors.

The activation of nucleophiles and electrophiles is contingent upon various factors, including the nature of the involved atoms, the presence of functional reactive groups, and reaction conditions. Offering a universal explanation for all nucleophilic and electrophilic reactions is challenging since they vary and depend on the specific context of the reaction.

It's worth noting that Mulliken charges can be employed to enhance the reactivity of atoms within a molecule, primarily in response to the interactions with nucleophiles or electrophiles. Atoms carrying positive charges are more susceptible to be electrophiles, while those with partial negative charges have a higher propensity to interact with the nucleophile.[20]

Table 2

Mulliken charge values of the atoms in the studied corrosion inhibitors, calculated at DFT/B3LYP/6-31G theoretical level

ISAO		**ISAS**	
Atom	**Charge**	**Atom**	**Charge**
C1	0.091642	C1	0.090675
C2	-0.311641	C2	-0.312073
C3	0.059315	C3	0.060586
C4	0.075882	C4	0.078972
C5	0.305998	C5	0.305410
C6	0.075139	C6	0.076051
Br7	0.138226	Br7	0.140892
C8	0.129465	C8	0.131637
C9	0.536971	C9	0.535829
N10	-0.713138	N10	-0.714721
C11	0.177491	C11	0.184024
C12	0.115021	C12	0.111982
C13	0.003829	C13	0.002309
C14	0.011038	C14	0.010962
C15	0.016475	C15	0.017007
C16	0.008881	C16	0.009903
C17	-0.039822	C17	-0.039532
N18	-0.428068	N18	-0.435265
C19	0.204276	C19	0.213276
C20	0.525470	C20	0.525083
N21	-0.355040	N21	-0.336277
C22	0.705829	C22	0.231945
N23	-0.089535	N23	-0.037869
O24	-0.426581	O24	-0.423373
O25	-0.404020	O25	-0.387675
O26	-0.413106	S26	-0.039757

The charge distribution can be further amplified through a method that prepares the central adsorbent device. In the context of corrosion inhibitors, a higher negative charge equates to a greater capacity to donate electrons. Mulliken charges and their distribution play a crucial role in preventing corrosion. Regions with the most negative charges are typically the primary sites for absorption. The atoms numbering across the studied molecular are shown in Fig. 4. According to Table 2, the C17 and N23 indicate the most favorable sites for interactions between ISAO corrosion inhibitor and the metal surface. However, the C17, N23 and S26 atoms exhibit higher negative charges and are predisposed to share electrons with the deficient metal surface.

Structure-Activity Relationship (SAR) Findings

Our investigation delved into the Structure-Activity Relationship (SAR) aspects, and the discerning outcomes obtained are thoughtfully presented in Table 3, elucidating essential factors that influence the anticorrosive properties of the studied molecules.

Table 3

SAR parameters of ISAO and ISAS corrosion inhibitors

SAR parameters	**ISAO**	**ISAS**
HE	-11.97	-14.55
log*P*	-1.13	0.68
V	1024.22	1058.41
SA	620.02	636.02
α	38.20	41.36

The polarizability (α) was meticulously calculated utilizing the HyperChem program package, characterizing the alterations in the electronic distribution of the molecule concerning the applied electric field. As polarization increases, the intrinsic molecular value also escalates, rendering the adsorption of the inhibitor molecule onto the metallic substrate a more facile process.[21] Notably, the results in Table 3 unequivocally demonstrate that ISAS boasts a higher polarizability (α) value compared to ISAO, which emphasizes the earlier reported inhibition efficacies.

In our exploration of hydrophobicity, designated by the partition coefficient (log*P*), we unveiled a parameter of significant importance in assessing a molecule's anticorrosive efficacy. Higher log*P* indicates higher degree of hydrophobicity which is translated into reduced water solubility, impeding the electronic transfer from the inhibitor to the metal surface and hampering the adsorption of the inhibitor molecule.[21] According to Table 3, log*P* obeys the order: ISAS > ISAO, which does not validate the experimental outcomes.

The hydration energy (HE) emerged as a critical facet in evaluating anticorrosive activity, with negative values indicating an exothermal dissolution of the studied molecule. Notably, an elevation in hydration energy directly correlates

with increased inhibition efficiency.[21] The (HE) data, as presented in Table 3, showcasing the sequence: ISAS < ISAO. This result is not in good accordance with the experimental order of the corrosion inhibition effectiveness earlier reported.

The surface area (SA) of the inhibitor molecule was another focal point in our SAR analysis, as it profoundly influences corrosion protection. A larger surface area facilitates enhanced contact between the inhibitor and the metallic surface resulting in a more efficacious inhibition.[21] The results collected in Table 3 solidify the understanding that ISAS has a larger surface area than ISAO, thereby promoting higher surface coverage and subsequently elevating inhibition efficiency. This observation aligns seamlessly with the experimental findings.

Lastly, we scrutinized the molecular volume (V) and its impact on the potential coverage of a metallic surface by the inhibitor. A larger molecular volume directly equates to a higher surface coverage, augmenting the protection provided to the metal surface by the inhibitor.[21] The comparison of molecular volume values across the studied structures affirms the trend: ISAS > ISAO, further corroborating the hierarchical efficacy of ISAS over ISAO, a concurrence with the experimental inhibition effectiveness data previously reported.

Toxicity prediction

The prediction of corrosion inhibitor toxicity holds paramount importance for a multitude of compelling reasons. Primarily, it serves as a crucial tool to safeguard the environment and ensure the well-being of human health and safety. Furthermore, it piques the keen interest of corrosion inhibitor manufacturers who aspire to engineer products that not only effectively combat corrosion but also exhibit a commendable commitment to environmental preservation and the protection of human health. The foresight into toxicity plays a pivotal role in the meticulous crafting of corrosion inhibitor formulations that prioritize safety and sustainability.[9] The toxicological parameters, encompassing carcinogenicity, skin sensitization, and AMES toxicity, have been meticulously predicted, and the results are thoughtfully presented in Table 4. Notably, the analysis reveals that the studied corrosion inhibitor candidates exhibit a remarkable profile, being devoid of carcinogenic properties, skin sensitization potential, and AMES toxicity.

Table 4

Predicted toxicity parameters of the studied isatin derivatives corrosion inhibitors

Parameter	ISAO	ISAS
Carcinogenicity	Inactive	Inactive
Skin sensitization	Safe	Safe
AMES toxicity	Safe	Safe

CONCLUSION

In the present study, comprehensive DFT investigations were conducted at the DFT/B3LYP/6-31G theoretical level. These investigations were complemented by Structure-Activity Relationship (SAR) analyses and toxicity assessments aimed at elucidating the behavior of the corrosion inhibitors under study, their molecular-level inhibition mechanisms, and the potential impact of these chemical compounds on human health. The following key findings emerge from our above discussions:

Global reactivity descriptors including E_{HOMO}, dipole moment, energy gap, hardness, and softness, exhibit a strong correlation with the observed experimental inhibition efficiency.

SAR parameters such as surface area, polarizability, and volume provide validation for the observed order of experimental inhibition efficiency, while the partition coefficient log*P* does not support this order.

Mulliken charge analysis offers compelling insights, unveiling a reactive scheme that highlights the active atomic sites responsible for electronic transfer.

The studied toxicological indices provide assurance regarding the safety of these inhibitors for human health.

These findings collectively enhance our understanding of the corrosion inhibitors' performance and safety implications at both the molecular level and in practical applications.

REFERENCES

1. M. I. Khan, A. Sarkar, H. K. Mehtani, P. Raut, A. Prakash, M. J. N .V. Prasad, I. Samajdar and S. Parida, *Mater. Chem. Phys.*, **2022**, *290*, 126623.
2. A. Bousskri, A. Anejjar, M. Messali, R. Salghi, O. Benali, Y. Karzazi, S. Jodeh, M. Zougagh, E. E. Ebenso and B. Hammouti, *J. Molec. Liquids*, **2015**, *211*, 1000–1008.
3. S. E. Hachani, Z. Necira, D. Mazouzi and N. Nebbache, *Acta Chim. Slovenica*, **2018**, *65*, 183–190.
4. A. Khiouani, S. E. Hachani, I. Selatnia, N. Nebbache and S. Makhloufi, *J. Indian Chem. Soc.*, **2022**, *99*, 100497.

5. O. M. A. Khamaysa, I. Selatnia, H. Zeghache, H. Lgaz, A. Sid, I. M. Chung, M. Benahmed, N. Gherraf and P. Mosset, *J. Molec. Liquids*, **2020**, *315*, 113805.
6. K. Abderrahim, O. M. A. Khamaysa, I. Selatnia and H. Zeghache, *Chem. Data Collections*, **2022**, *39*, 100848.
7. M. A. Mostafa, A. M. Ashmawy, M. A. M. AbdelReheim, M. A. Bedair and A. M. Abuelela, *J. Molec. Struct*., **2021**, *1236*, 130292.
8. P. P. Zamora, K. Bieger, A. Cuchillo, A. Tello and J. P. Muena, *J. Molec. Struct.*, **2021**, *1227*, 129369
9. C. M. Fernandes, M. V. Palmeira-Mello, M. C. Leite, J. A. M. Oliveira, I. I. Martins, R. G. de Sá, L. A. de Almeida, A. M. T. Souza, V. R. Campos and E. A. Ponzio, *Mater. Chem. Phys.*, **2022**, *290*, 126508.
10. R. M. Kubba, M. M. Kazem, S. M. Al-Majidi and A. A. M. Ali, *JAIEM*, **2016**, *5*, 28–44.
11. H. Bourzi, R. Oukhrib, B. El Ibrahimi, Hi. Abou Oualid, Y. Abdellaoui, B. Balkard, M. Hilali and S. El Issami, *Surface Sci.*, **2020**, *702*, 121692.
12. S. C. Liu, X. R. Zhu, D. Y. Liu and D. C. Fang, *Phys. Chem. Chem. Phys.*, **2023**, *25*, 913–931.
13. T. Koopmans, *Physica E*., **1934**, *1*, 104–113.
14. R. G. Pearson, *Inorg. Chem*., **1988**, *27*, 734–740.
15. R. G. Pearson, *J. Chem. Edu*., **1987**, *164*, 561.
16. K. Ramya, R. Mohan, K. K. Anupama and A. Joseph, *Mater. Chem. Phys*., **2015**, *149-150*, 632–647.
17. I. B. Obot and Z. M. Gasem, *Corros. Sci.*, **2014**, *83*, 359–366.
18. A. Bouoidina, F. El-Hajjaji, Abdellaoui, Z. Rais, M. Filali Baba, M. Chaouch, O. Karzazi, A. Lahkimi and M. Taleb, *JMES*, **2017**, *8*, 1328–1339.
19. I. Lukovits, E. Kalman and F. Zucchi, *Corrosion*, **2001**, *57*, 3–8.
20. A. Dutta, K. S. Saha, P. Banerjeeb and D. Sukul, *Corros. Sci*., **98**, 541–550.
21. A. M. Al Sabagh, N. M. Nasser, A. A. Farag, M. A. Migahed, A. M. F. Eissa and T. Mahmoud, *Egypt. J. Petrol.*, **2013**, *22*, 101–116.